



NRL/MR/5651--17-9712

Frequency Dependent Harmonic Powers in a Modified Uni-Traveling Carrier (MUTC) Photodetector

YUE HU

*University of Maryland
Baltimore, Maryland*

MEREDITH N. HUTCHINSON

*Photonics Technology Branch
Optical Sciences Division*

CURTIS R. MENYUK

*University of Maryland
Baltimore, Maryland*

January 27, 2017

CONTENTS

I	EXECUTIVE SUMMARY	E-1
II	INTRODUCTION	1
III	SIMULATION RESULTS	1
IV	DISCUSSION	7
V	SUMMARY	11
VI	REFERENCES	12

I EXECUTIVE SUMMARY

We use a drift-diffusion model to study frequency dependent harmonic powers in a modified uni-traveling-carrier (MUTC) photodetector. The model includes external loading, incomplete ionization, the Franz-Keldysh effect, and history-dependent impact ionization. It also takes into account heat flow in the device. In three-tone measurements, the bias voltage at which a null occurs (bias null) in the second order intermodulation distortion (IMD2) is different for the sum frequency and difference frequency. We obtained agreement with the experimental results. The bias null that appears in the IMD2 is due to the Franz-Keldysh effect. The bias null depends on the electric field in the intrinsic region, and the difference of the bias null for the sum frequency and difference frequency are due to the displacement current in the intrinsic region. When the frequency is large, the displacement current is large and has a large effect on the harmonic powers. We also found that the bias null depends on the recombination rate in the *p*-absorption region because the electric field decreases in the intrinsic region when the recombination rate in the *p*-region decreases.

II INTRODUCTION

Asymmetries in the amplitudes of lower and upper intermodulation distortion (IMD) tones are often observed in microwave devices that are subjected to two-tone or three-tone tests. These asymmetries are also observed in the photodetector measurement [1, 2]. In a three-tone measurement, where the modulation frequencies are F_1 , F_2 , and F_3 , the IMD power that is associated with the frequency combination $F_1 + F_2$ is different from the one at $|F_1 - F_2|$. In particular, the bias voltage at which a null occurs (bias null) in the IMD is different. The frequency dependence of the IMD power may be due to a memory effect, i.e., a bandwidth-dependent nonlinear effect. There are several studies of the memory effect on a microwave amplifier [3, 4], but the physical reason for the IMD power difference in a photodetector remains unclear. In this report, we will use the drift-diffusion model to determine which factors contribute to the memory effect in an MUTC photodetector.

Figure 1 show the structure of the MUTC photodetector [5]. The main difference between this structure and a UTC photodetector is that there is a cliff layer between the collection layer and the absorption layer. The cliff layer is moderately doped. Without the cliff layer, the electric field is present throughout the entire intrinsic region. With a cliff layer, the electric field is mostly present in the InGaAs intrinsic layer instead of the entire intrinsic region. The electric field in the InGaAs intrinsic layer increases due to the cliff layer, which reduces the space charge effect. Another difference is that there is a thin intrinsic layer of InGaAs, which is used to increase the responsivity. InGaAsP layers were placed between the InP and InGaAs layers to help electrons transfer easily from InGaAs to InP, due to a decrease in the gap between the conduction bands.

A three-tone setup [6] was used to measure the harmonic powers in the device. The device output power was measured as a function of reverse bias voltage from 0–10 V in 0.25 V increments. The frequencies are 4.9 GHz, 5.0 GHz, and 5.15 GHz. The average photocurrent is 20 mA. We show the experimental results in Fig. 3. We can separate the IMD2 (second-order IMD powers) into two groups. One group contains the sum frequencies powers at $F_1 + F_2$, $F_1 + F_3$, and $F_2 + F_3$, and the other group contains the difference frequencies powers at $|F_1 - F_2|$, $|F_1 - F_3|$, and $|F_2 - F_3|$. In each group, the IMD2 behavior is the same. Hence, we only show the IMD2 powers at $F_1 + F_2$ and $|F_1 - F_2|$. However, we observe a significant difference between the IMD2 powers for the sum frequency ($F_1 + F_2$) and the difference frequency ($|F_1 - F_2|$). A bias null appears in both IMD2 powers, but the bias voltage at which a null appears is different.

III SIMULATION RESULTS

We used a drift-diffusion model to study IMD in this MUTC device [5]. We use a three-tone setup, which is same as in the experiments. The generation rate may be expressed as

$$G = G_0 \{1 + m_d [\sin(2\pi F_1 t) + \sin(2\pi F_2 t) + \sin(2\pi F_3 t)]\}, \quad (1)$$

where G_0 is the steady state generation rate, m_d is the modulation depth, and F_1 , F_2 , and F_3 are the three-tone modulation frequencies.

Figure 4 shows the steady-state electron and hole currents in the device. We see that in the n -region, the total current depends on electron current, and in the p -region, the hole current is larger than the electron current. In the intrinsic region, the electron current is larger than the hole current. We know that the response time of the MUTC device depends mainly on the electron transit time. It is important to analyze the electron current in the intrinsic region, where most of the electrons are generated.

We show the simulation results for the IMD2 power in Fig. 5, and the agreement with the experiments is good. We also obtain a bias null in the IMD2 power. The bias null in the difference frequency IMD2 power

InGaAs, p+, Zn, 2.0×10^{19} , 50nm	50 nm
InP, p+, Zn, 1.5×10^{18} , 100nm	150 nm
InGaAsP, Q1.1, Zn, 1.0×10^{16} , 15nm	165 nm
InGaAsP, Q1.4, Zn, 1.0×10^{16} , 15nm	180 nm
InGaAs, p, Zn, 2.0×10^{18} , 100nm	280 nm
InGaAs, p, Zn, 1.2×10^{18} , 150nm	430 nm
InGaAs, p, Zn, 8.0×10^{17} , 200nm	630 nm
InGaAs, p, Zn, 5.0×10^{17} , 250nm	880 nm
InGaAs, Si, 1.0×10^{16} , 150nm	1030 nm
InGaAsP, Q1.4, Si, 1.0×10^{16} , 15nm	1045 nm
InGaAsP, Q1.1, Si, 1.0×10^{16} , 15nm	1060 nm
InP, Si, 1.4×10^{17} , 50nm	1110 nm
InP, Si, 1.0×10^{16} , 900nm	2010 nm
InP, n+, Si, 1.0×10^{18} , 100nm	2110 nm
InP, n+, Si, 1.0×10^{19} , 900nm	3010 nm
InGaAs, n+, Si, 1.0×10^{19} , 20nm	3030 nm
InP, n+, Si, 1.0×10^{19} , 200nm	3230 nm
InP, semi-insulating substrate Double side polished	

Fig. 1: Structure of the MUTC photodetector. Green indicates the absorption regions, which include an intrinsic region and a *p*-doped region. Red indicates highly doped InP layers, purple indicates highly-doped InGaAs layers, and white indicate other layers.

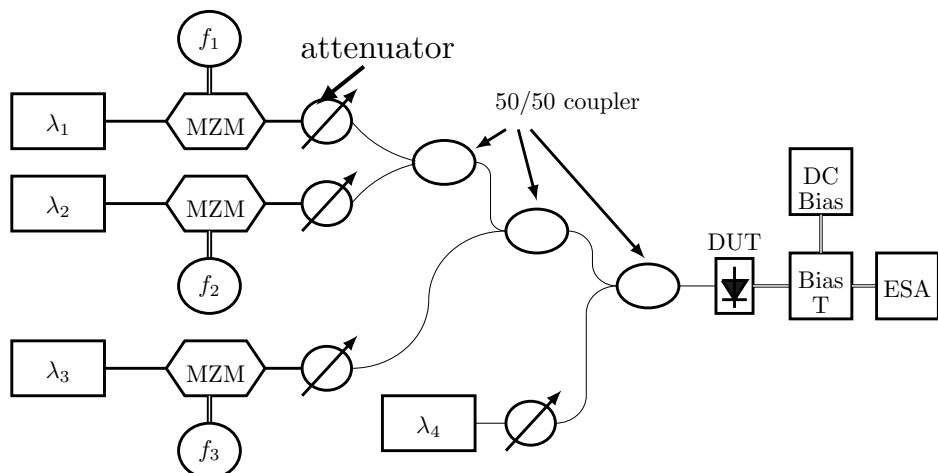


Fig. 2: Schematic illustration of the test setup. MZM = Mach-Zehnder modulator, DUT = Device under test, ESA = Electronic spectrum analyzer

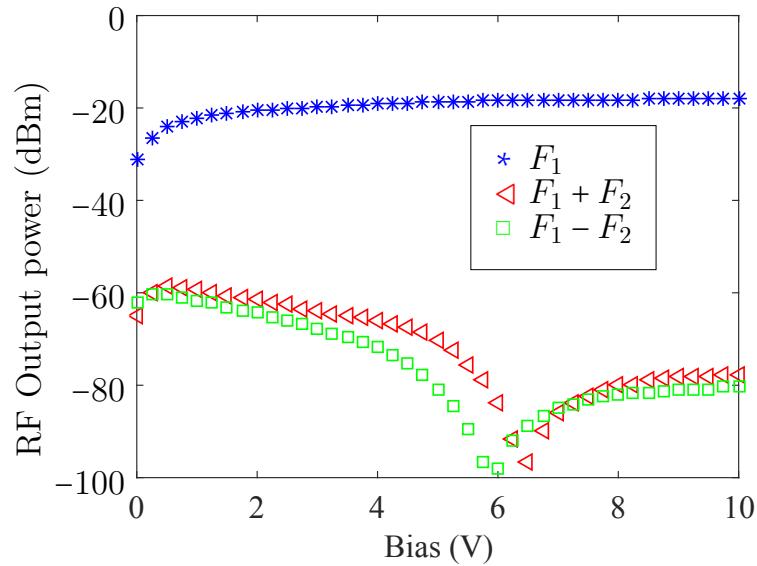


Fig. 3: The measured fundamental, IMD2, and IMD3 powers as a function of reverse bias for input frequencies $F_1 = 4.9$ GHz, $F_2 = 5.0$ GHz, and $F_3 = 5.15$ GHz with a photocurrent of 20 mA.

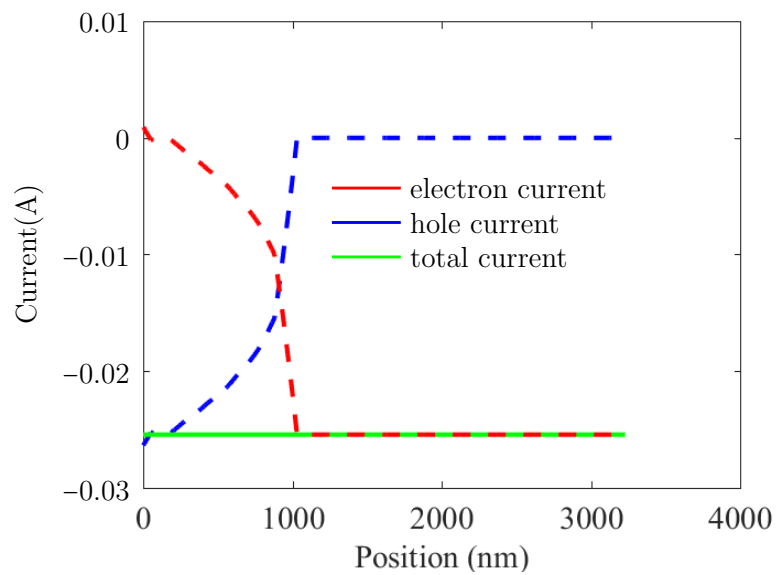


Fig. 4: The calculated electron and hole currents in the device.

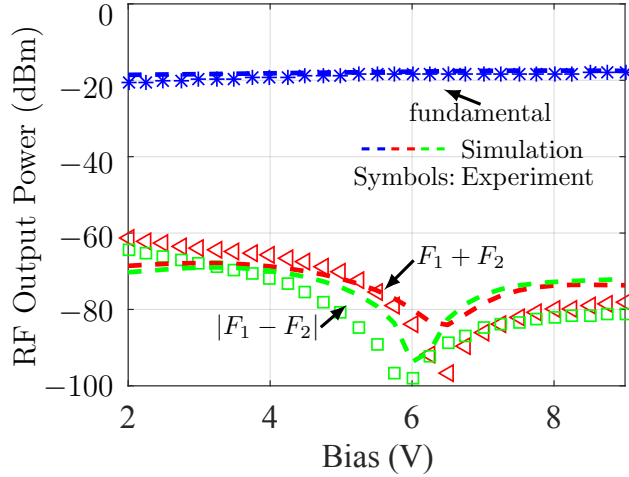


Fig. 5: The measured and calculated fundamental and IMD2 powers as a function of reverse bias for input frequencies $F_1 = 4.9$ GHz, $F_2 = 5.0$ GHz, and $F_3 = 5.15$ GHz.

appears at around 6 V, while the bias null in the sum frequency IMD2 power appears at around 6.5 V, which agrees with the experiment.

Figure 6 shows the RF output power when the Franz-Keldysh effect is not included. We found that there is no bias null in the IMD2 power. We conclude that the nulls are due to the Franz-Keldysh effect. The absorption coefficient changes when the electric field changes in the device, so that the generation rate in the device — especially in the intrinsic absorption region — changes as a function of electric field. The nulls appear at biases where the change of absorption coefficient as a function of the electric field strength is small. Figure 7 shows the electric field at 2 and 6 V. We see that the electric field only differs significantly from zero in the intrinsic absorption region, which is due to the cliff layer. The Franz-Keldysh effect changes the absorption in the intrinsic absorption region since the electric field is large. Figure 8 shows the absorption coefficient as a function of the electric field. When the electric field is around 150 kV/cm, which correspond to an applied bias of 6 V, the absorption reaches its peak. However, at this electric field, the change of absorption due to the change of the electric field is small, so that the nonlinearity due to the Franz-Keldysh effect is minimized. Hence, the IMD2 power reaches its lowest value around 6 V.

Figure 9 shows the current output in the presence of three-tone modulation and one-tone modulation. With three-tone modulation, it is difficult to determine the physical origin of the device nonlinearity and explain the origin and location of bias null because two or three frequencies are mixed together. We will use the one-tone modulation to analyze the physical origin of the nonlinearity. We will show that the results with three-tone modulation and a simulation that keeps only one tone are almost the same. Figure 10 shows the electron density as a function of time compared to a modulation sine function (one-tone modulation) in the intrinsic region. The amplitude of the modulation sine function is adjusted to have the same amplitude as the electron density, but the phase is unchanged. We observe that the electron density is not exactly a sine function. It is a delayed with respect to the modulation sine function. We also find that the modulation depth for the electron density (about 0.19) is larger than the modulation depth (0.04) of the optical input power, which becomes the electron in the intrinsic region. This increase in the modulation depth occurs because electrons accumulate in the intrinsic region at the heterojunction boundary with the cliff layer. In Fig. 10(a), we show that the difference of the electron density from the sine function at 5 V is larger than the difference of the electron density from the sine function at 6 V, which occurs because the Franz-Keldysh

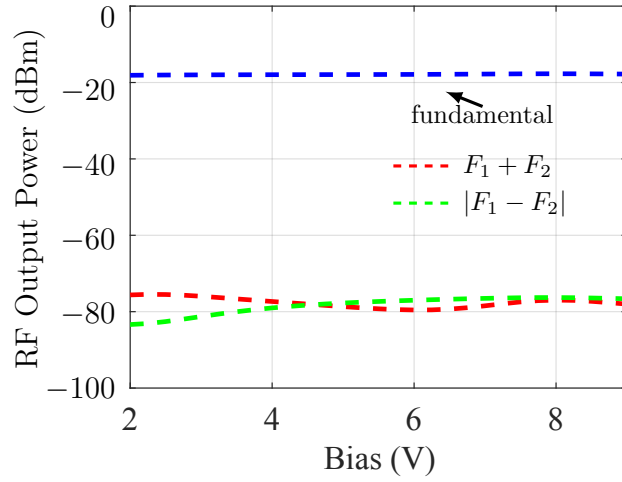


Fig. 6: The calculated fundamental and IMD2 powers as a function of reverse bias for input frequencies $F_1 = 4.9$ GHz, $F_2 = 5.0$ GHz, and $F_3 = 5.15$ GHz. The Franz-Keldysh effect is not included in the simulation.

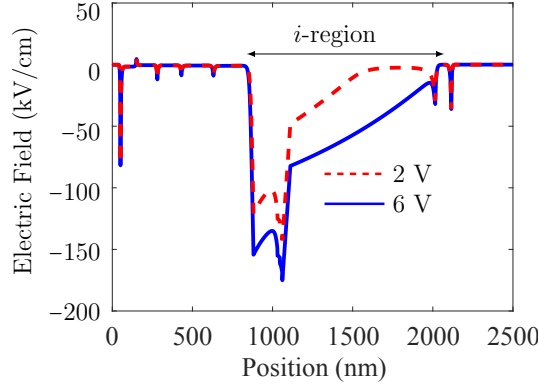


Fig. 7: The calculated electric field in the device at 2 and 6 V.

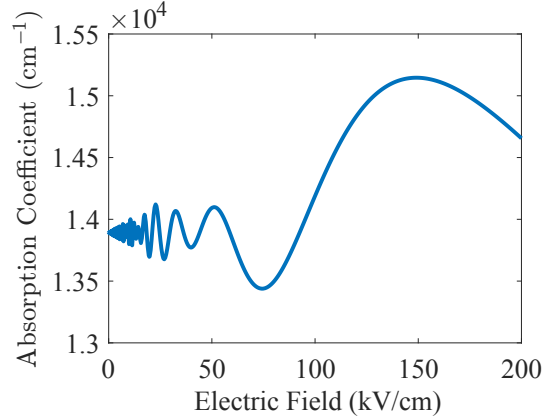


Fig. 8: The calculated absorption coefficient as a function of the electric field strength.

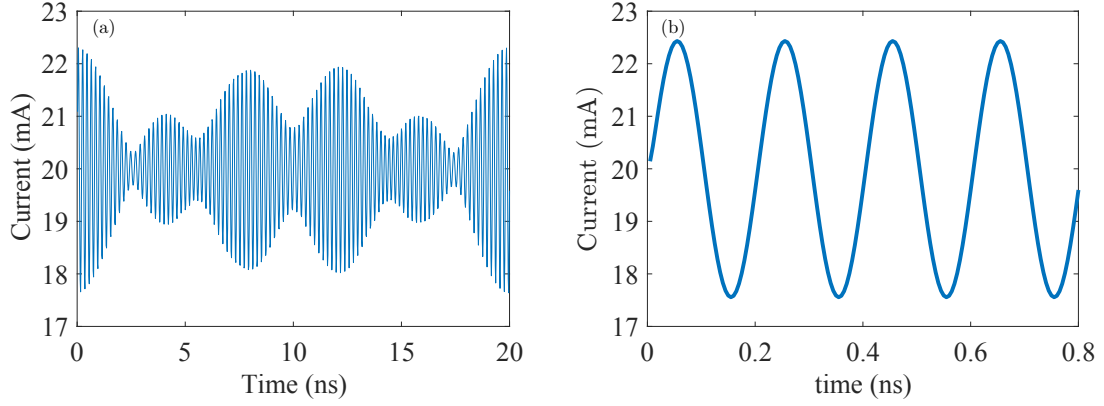


Fig. 9: The current output of the photodetector with (a) three-tone and (b) one-tone modulation.

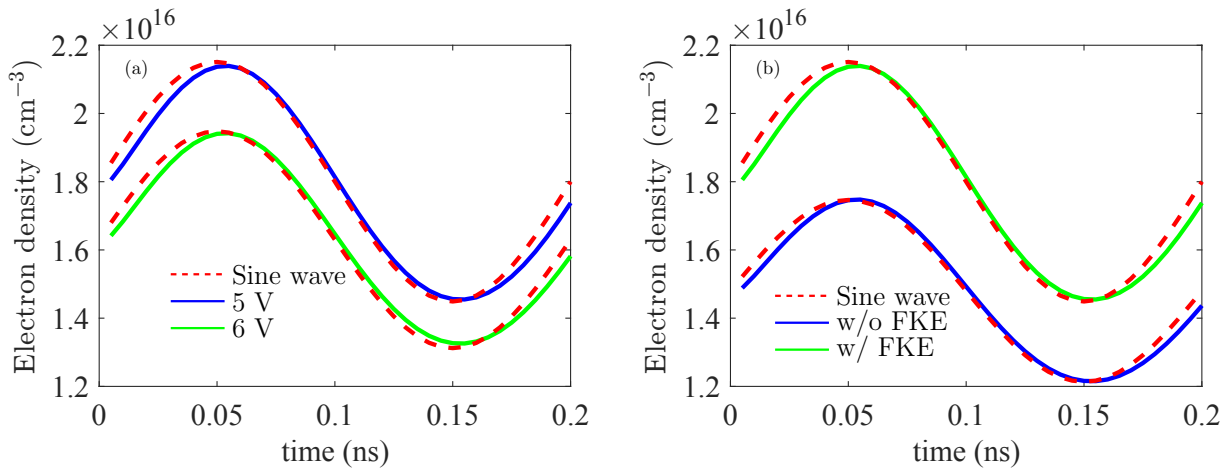


Fig. 10: (a) The calculated electron density in the intrinsic region at 1000 nm compared to a sine function at 5 and 6 V. (b) The calculated electron density in the intrinsic region at 1000 nm compared to a sine function with and without the Franz-Keldysh effect (FKE).

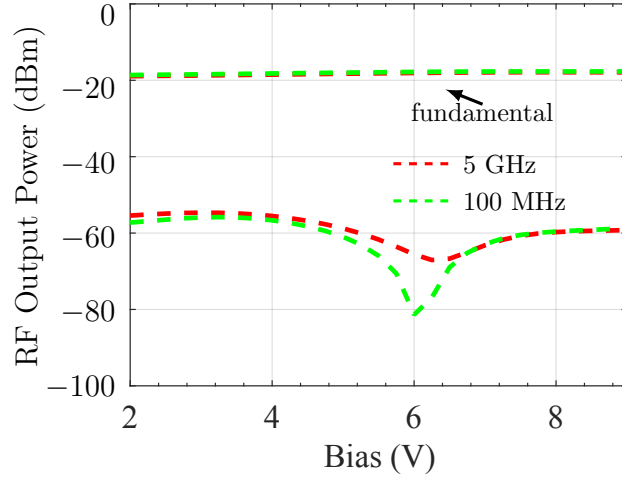


Fig. 11: The calculated RF output powers for modulation frequencies of 100 MHz and 5 GHz.

effect is mitigated when the bias is 6 V, as we previously discussed. Figure 10(b) shows the electron density as a function of time with and without the Franz-Keldysh effect at 5 V. We observe that difference between the electron density and the sine function is larger when the Franz-Keldysh effect is taken into account, providing for further evidence that the Franz-Keldysh effect is the principle source of nonlinearity in the device.

We have shown that the Franz-Keldysh effect is the reason for the null that appears in the IMD2 power, but we have not explained why the null position is different for the sum frequency and the difference frequency IMD2 powers. We use a one-tone simulation with different modulation frequencies to examine this question. The modulation frequencies are set to 100 MHz and 5 GHz, so that the second-order frequencies are 200 MHz and 10 GHz, which correspond to the difference and sum frequencies in the three-tone measurement. We show the harmonic powers in Fig. 11. We see that the bias null in the second-order harmonic power at a modulation frequency of 100 MHz is the same as the bias null in the three-tone simulation at frequency $|F_1 - F_2|$, and the bias null in second-order harmonic power at a modulation frequency of 5 GHz is the same as the bias null in the three-tone simulation at frequency $F_1 + F_2$. This frequency dependence of the null position is consistent with experiments.

IV DISCUSSION

The current in the intrinsic region includes the electron current, the hole current, and the displacement current. We show these currents in Fig. 12 at 5 GHz. We see that the displacement current is almost zero at all positions except in the intrinsic region. Although the displacement current is small compared to the electron and hole currents in the intrinsic region, the displacement current contributes to the harmonic powers. In Fig. 13(a), we show the RF output current in the intrinsic region without the displacement current. We find that the bias nulls are the same for different modulation frequencies. Displacement current is responsible for the difference in the bias null for the sum and difference frequencies IMD2 powers. The displacement current depends on the changes of electric field in the intrinsic region. When the modulation frequency is large, the change of electric field increases, and the displacement becomes large and has a large effect on the harmonic powers. Figure 13(b) shows the IMD2 power of the displacement current. At the sum frequency

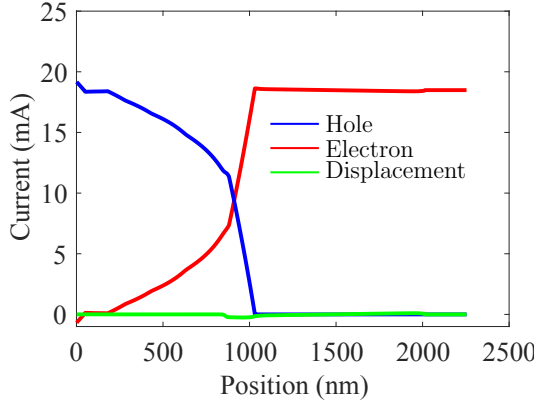


Fig. 12: The calculated amplitude of the electron, hole, and displacement current in the device when a modulation is applied at 5 GHz.

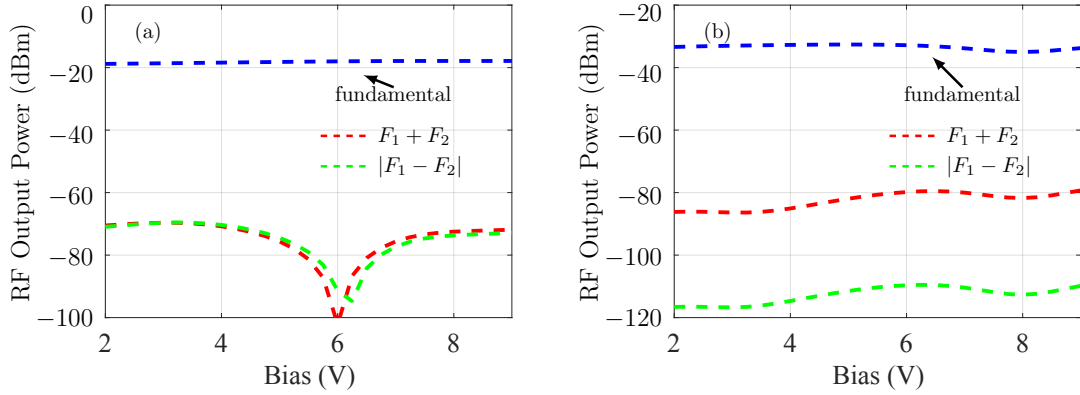


Fig. 13: The calculated fundamental and IMD2 powers as a function of reverse bias for input frequencies $F_1 = 4.9$ GHz, $F_2 = 5.0$ GHz, and $F_3 = 5.15$ GHz. (a) Displacement current is not included in the total current. (b) IMD2 power of the displacement current

$F_1 + F_2$, the IMD2 power of the displacement current is around -85 dBm, which is close to the IMD2 power of the total current. While the IMD2 power of the displacement current at the difference frequency $|F_1 - F_2|$ is about -125 dBm, which is much smaller than the IMD2 power of the total current. So, the displacement current does not affect the IMD2 power of the difference frequency.

From a circuit perspective, the displacement current is due to device capacitance. Charge of opposite sign on each side of the intrinsic region, and there is almost no charge in the intrinsic region, creating a capacitor. We show the charge in the p -region and intrinsic region in Fig. 14. We see that when the bias increases, the charge in the p -region increases. We note that the charge in the p -region is negative and is positive in the n -region. Figure 15 shows the capacitance of the device as a function of bias. The capacitance in the photodetector is almost constant when the bias is large, but the impedance of the capacitance is different for different modulation frequencies. The impedance difference for different modulation frequencies leads to different displacement currents, which affects the bias null in the IMD2. Figure 16 shows the largest displacement current when modulation is applied to the device for modulation frequencies of 200 MHz and 5 GHz. We observe that the displacement current with a 5 GHz modulation is much larger than with a 200

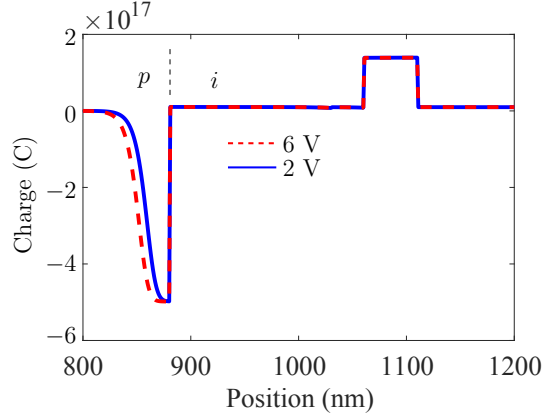


Fig. 14: The calculated charge in the *p*-region and intrinsic region in the device at 2 and 6 V.

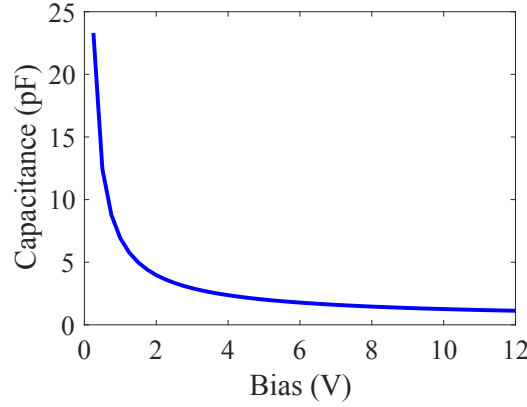


Fig. 15: The calculated capacitance in the device as a function of bias.

MHz modulation. The displacement current is larger in the intrinsic absorption region, where the electric field is larger than it is in other regions.

Figure 17 shows the three-tone RF output powers as a function of applied bias, when the lifetime increases from 1×10^{-11} s to 5×10^{-11} in the *p*-region. We found that the null position in the second order harmonic powers are almost the same for the sum frequency and the difference frequency. The recombination rate in the *p*-region is important to determine the bias null of the IMD2. When the recombination time increases, the recombination rate decreases in the *p*-region, so that more electrons enter the intrinsic region, increasing the electron density and decreasing the electric field in the intrinsic region. We have shown that the Franz-Keldysh effect causes the null to appear when the electric field is around 150 kV/cm. So, when the electric field decreases due to the increase in the electron lifetime in the *p*-region, the bias null moves to a larger voltage bias where the average electric field in the intrinsic absorption region is around 150 kV/cm.

We also found that the electron diffusion coefficient is a factor in determining the position of the nulls. When the diffusion coefficient of the electrons in the *p*-region increases, more electrons diffuse into the *p*-region, so that the electric field in the intrinsic region increases, and the capacitance increases, which leads to smaller impedances for high modulation frequencies.

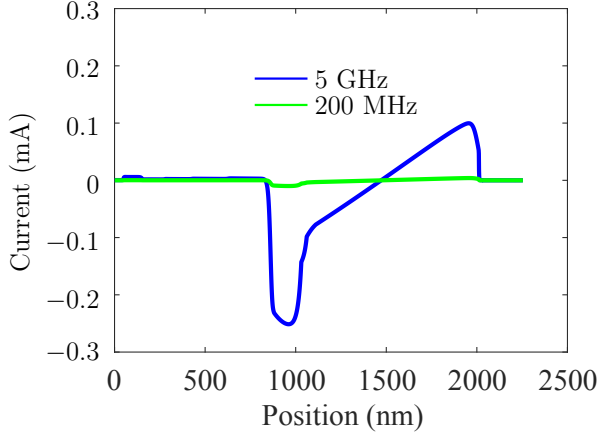


Fig. 16: The amplitude of the sinusoidally varying displacement current in the device at 200 MHz and 5 GHz.

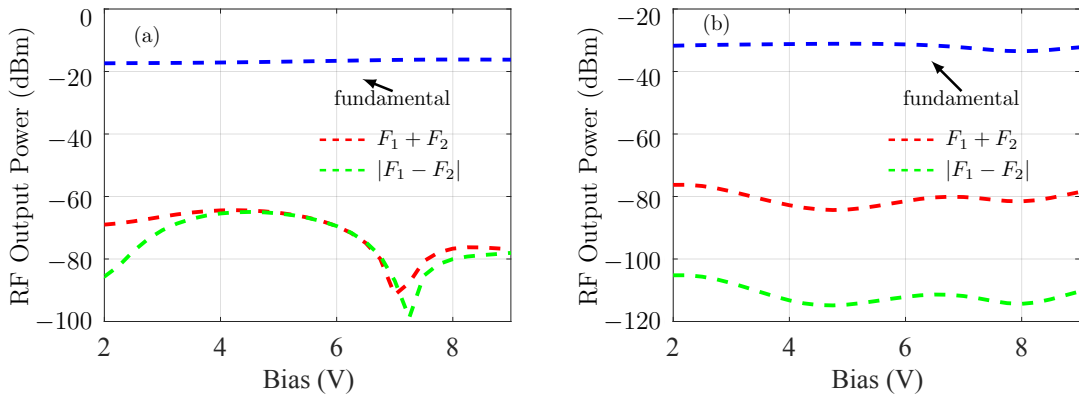


Fig. 17: The calculated fundamental and IMD2 powers as a function of reverse bias for input frequencies $F_1 = 4.9$ GHz, $F_2 = 5.0$ GHz, and $F_3 = 5.15$ GHz. The lifetime in the p -region is 5×10^{-11} s.

V SUMMARY

We obtained agreement with experiments for the null position in the IMD2 power for different modulation frequencies. We investigated the physical origin of the nulls in the IMD2 power and we found that the Franz-Keldysh effect causes the bias nulls. The difference in the location of the bias nulls between the sum frequency and difference frequency IMD2 powers is due to the displacement current in the intrinsic region. When the frequency is high, the displacement current is large and affects the harmonic powers.

We also found that the recombination rate in the p -region affects the bias null in the IMD2 power. When the recombination rate decreases, more electrons enter into the intrinsic region, which decreases the electric field in this region. Then the bias null moves to a higher bias. The diffusion coefficient in the p -region is also a factor in determining the location of the bias null.

VI REFERENCES

- [1] M. N. Hutchinson and V. J. Urivk, “Memory dependent distortion in photodetectors.” Unpublished paper, 2016.
- [2] N. J. Frigo, M. N. Hutchinson, and J. R. Peasant, “Characterization of photodiode nonlinearities by output frequency analysis,” *J. Lightw. Technol.*, in press.
- [3] N. B. D. Carvalho and J. C. Pedro, “Large- and small-signal imd behavior of microwave power amplifiers,” *IEEE Trans. Microw. Theory Techn.*, vol. 47, no. 12, pp. 2364–2374, 1999.
- [4] N. B. D. Carvalho and J. C. Pedro, “A comprehensive explanation of distortion sideband asymmetries,” *IEEE Trans. Microw. Theory Techn.*, vol. 50, no. 9, pp. 2090–2101, 2002.
- [5] Z. Li, H. Pan, H. Chen, A. Beling, and J. C. Campbell, “High-saturation-current modified uni-traveling-carrier photodiode with cliff layer,” *IEEE J. Quantum Electron.*, vol. 46, no. 5, pp. 626–632, 2010.
- [6] M. N. Draa, A. S. Hastings, and K. J. Williams, “Comparison of photodiode nonlinearity measurement systems,” *Opt. Express*, vol. 19, no. 13, pp. 12635–12645, 2011.